An investigation of the 2D and 3D Ising Models

Candidate number: 26812
Department of Physics, University of Bath, Bath BA2 7AY, United Kingdom
Date submitted: 27 Apr 2025

Abstract

The Ising model (IM) provided a valuable framework for studying phase transitions, magnetism, and related phenomena. The Metropolis Monte Carlo method was used to simulate the two dimensional square lattice IM in C++, with periodic boundary conditions taken to ensure spin interactions at the boundaries. Energy, magnetism, heat capacity, and magnetic susceptibility were computed throughout the simulation. There was good conformity to Onsager's exact solution for energy, with slight discrepancies in magnetism and heat capacity. Magnetic susceptibility was shown to increase with system size, proving computational methods to be imperfect. By observing at which temperature phase change occurred, the critical temperature (T_c) was correctly estimated to be $T_c \approx 2.269$. Mean field theory (MFT) was shown to be mostly inaccurate for the 2D IM, although it correctly estimated behaviour around T_c. The correlation function was also investigated, where long range order was observed for temperatures close to the T_c. Additionally, the analysis was extended to the three dimensional Ising model (3D IM), for which no exact solution exists. Results showed a clear phase transition at $T_0^{3D} \approx 4.5$, which is the estimated critical temperature of the 3D IM (T_c^{3D}). The behaviour of the simulated 3D IM was similar to predictions from MFT around T_c^{3D}, validating the simulated results.

1 Introduction

The Ising model (IM) is a fundamental mathematical model used to describe phenomena such as phase transitions and magnetism in materials. It comprises a lattice of spins, each of which can be in one of two states: up (+1) or down (-1). Spins interact with their nearest neighbours; the nature of these interactions is influenced by the temperature of the system. The overall spin alignment across the lattice determines macroscopic properties such as magnetism and energy.

The IM is exactly solvable in 1D and the 2D square lattice, as shown in the work of Ising and Onsager, respectively [Ising, 1925] [Onsager, 1944]. Notable results from Onsager's exact solution of the 2D IM are: the behaviour of magnetism, energy, heat capacity, and magnetic susceptibility for varying temperature; and the critical temperature (T_c) where the IM undergoes a second-order phase transition [Rostami, 2025]. This critical temperature is given by

$$T_c = \frac{2J}{k_B \ln(1+\sqrt{2})} \approx 2.269 \frac{J}{k_B}. \tag{1}$$

To simplify computations the interaction term, J, and Boltzmann's constant, k_B, are both taken as 1, which gives a proportionate temperature,

$$T_0 = \frac{J}{k_B} T. \tag{2}$$

This gives the dimensionless value, $T_c \approx 2.269$.

Unlike the 1D and (square) 2D Ising model, exact solutions are not known for higher-dimensional or more complex configurations, such as the three dimensional Ising model (3D IM). Comparing numerical estimations with results from the known solutions provides a means to validate computational methods. The same computational methods can then be extended to more complex systems, providing estimations for the behaviour of the IM in unsolved configurations.

Mean field theory (MFT) gives an approximation for the behaviour of the properties of the IM. However, the accuracy of these approximations suffers in 2D, greatly deviating from exact solutions near the critical temperature. MFT proves particularly useful for validating the results of the 3D IM, since there is no exact solution.

Real world applications of the 3D IM include:
- Studying magnetic thin films; useful in the research and development of hard disk drives.
- Understanding the way amino acids interact and fold into their functional structures; helping researchers understand diseases like Alzheimer's.
These give motive to investigate the 3D case, and to ensure that estimations are as accurate as possible.

2 Computational methods

The 2D square IM grid was emulated in C++ using an array of pointers of size *gridsize*. Each element of this array was also assigned as a array of size *gridsize*, representing one row. The total number of spins in the IM is then $N = gridsize^2$. Computational constraints led to *gridsize* being taken as 250, and hence $N = 250^2 = 62500$.

Periodic boundary conditions were taken using modular arithmetic, which simplified finding spin neighbours at boundaries. Initially, all spins were set to down, which was represented by assigning each position of the grid a value of -1. The ***nupengl*** library was used to visualise this, where blue and green squares represent the up and down spins respectively (see Figure 1). To increase efficiency, computations were run in parallel, using six different seeds to ensure results were independent.

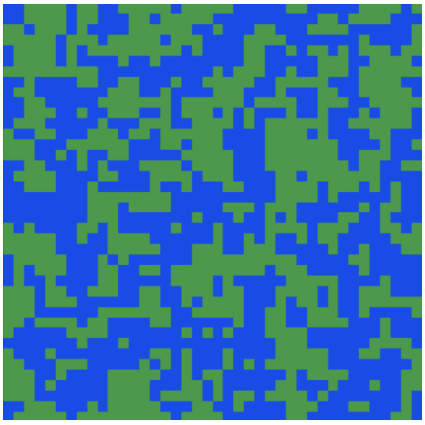

Figure 1: 2D square lattice IM at equilibrium using ***nupengl*** library, $gridsize = 40$, $T_0 = 4$. Blue and green represent up and down spins respectively.

2.1 Metropolis Monte Carlo sweep

To update the spins in the system, the Metropolis Monte Carlo (MC) method was applied. Here, a spin is picked at random and the change in system energy, ΔE, that would occur if that spin changed its polarisation is calculated. Total energy of the IM can be written as:

$$E = \frac{1}{2}\sum_i E_i, \tag{3}$$

with E_i representing local energy for some spin i. Therefore the change in total energy, $\Delta E = E_{\text{initial}} - E_{\text{final}}$, is equivalent to the change in the local energy for the picked spin. This is calculated with:

$$\Delta E_i = -2 \sum_{j \text{ n.n. of } i} J s_i s_j, \tag{4}$$

where n.n. stands for nearest neighbours and J is the interaction term, which describes the strength of the interaction between neighbouring spins.

If $\Delta E_i \leq 0$ (energy decreases) then this change is accepted, and the spin flips. If $\Delta E_i > 0$ (energy increases) then this change is accepted with probability $p = e^{-\Delta E_i / k_B T}$. Otherwise the change is rejected and the spin is left in its original state. One MC sweep performs N attempted spin flips.

For two dimensions, this is a remarkably simple procedure. For any chosen spin with its respective neighbours, there are only five distinct scenarios (see Figure 2). Firstly (1), there is the case where all neighbouring spins share the same polarisation as the chosen spin. In this case, the spin will flip with a probability of e^{-8/T_0}. Another case (2) is where three of the four neighbours share the same polarisation as the chosen spin. This will give a probability of e^{-4/T_0} to flip. Since $\Delta E \leq 0$ for each of the last three configurations (3, 4 and 5), the spin will flip whenever any of these cases are considered.

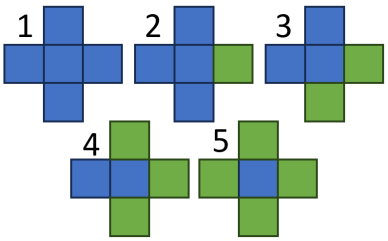

Figure 2: All possible configurations of local spin neighbours, considering the symmetry of up and down spins; and the invariance of ΔE_i from neighbour position.

2.2 Properties of the Ising model

The IM has many properties, including: magnetism (M), energy (E), magnetic susceptibility (χ), and heat capacity (c). Magnetism can be found by summing over all spins in the system, which is then normalised by dividing by N. Energy per spin is computed by summing the product of all four of the nearest neighbour pairs, and again normalising by dividing by N. Estimates of magnetic susceptibility and heat capacity can be found by computing the variance in magnetism and energy respectively.

$$E = \frac{1}{N}\sum_{\langle i,j \rangle} s_i s_j \quad \text{(5a)} \qquad M = \frac{1}{N}\sum_i s_i \quad \text{(5b)}$$

$$c = \frac{1}{NT_0^2}\text{Var}(E) \quad \text{(5c)} \qquad \chi = \frac{N}{T_0}\text{Var}(M) \quad \text{(5d)}$$

Magnetism and energy were both directly calculated in C++ using (5a) and (5b) respectively. The variances of magnetism and energy were calculated in R using the inbuilt variance function. These were used to find values of heat capacity and magnetic susceptibility using (5c) and (5d) respectively.

2.3 The correlation function

An interesting property of the IM is the correlation function which measures how strongly two spins are related. It is calculated using

$$G_{ij} = \langle s_i s_j \rangle, \tag{6}$$

where s_i and s_j are a certain distance apart. There are only two results for the correlation function for any spin pairs. If the two spins are both positive, then the correlation function for that pair will be $1 \times 1 = 1$, and likewise for if both spins are negative; $-1 \times -1 = 1$. If the two spins are of opposite sign, then the correlation function will be $1 \times -1 = -1$. This means the correlation function will take average values between -1 and 1, with a value of 1 indicating high correlation between neighbouring spins and 0 indicating no correlation. A value of -1 would also indicate high correlation, but it would imply that the spins are more likely to be opposite to their neighbours.

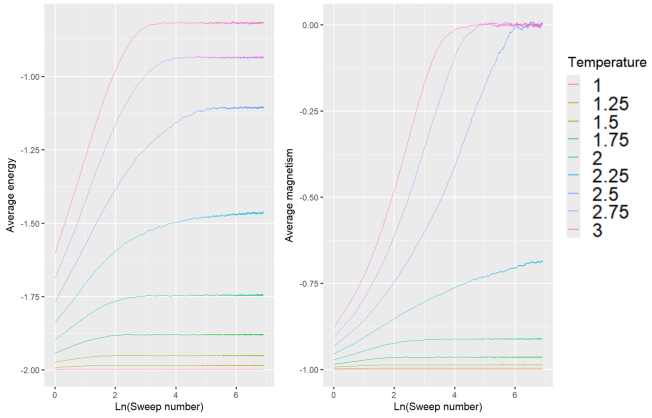

Figure 3: Average energy and magnetism against ln(Sweep number) for 9 different temperatures. Produced with 1000 sweeps, $gridsize = 250$, 30 repeats.

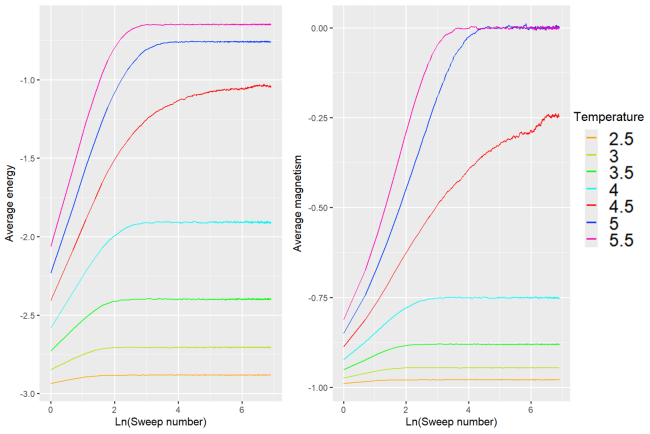

Figure 4: Average energy and magnetism against ln(Sweep number) for the 3D IM, 1000 sweeps, grid size 40, 30 repeats, 7 different temperatures. $T_0^{3D} = 4.5 \approx T_c^{3D}$ highlighted in red.

2.4 The three dimensional Ising model

While the 2D IM provides some insight into magnetic dynamics, the extension of the model into three dimensions presents a more complex and realistic representation of physical systems, such as ferromagnetic materials. Unlike the 2D IM, the 3D case lacks a known exact solution, making numerical simulations essential for studying the system's properties.

To simulate the 3D IM, a third dimension was added to the grid array in the C++ code. This meant that the functions to compute M, E, and correlation had to be rewritten to sum over the third dimension.

The MC sweeps are performed similarly in the 3D IM as they were for the 2D IM, but now the system exhibits more complicated behaviour due to the increased number of neighbours. Each spin now has six nearest neighbours, one in each direction along the x, y, and z axes. This increases the number of configurations shown in Figure 2 from 5 to 7.

A limitation of modelling the 3D IM is that there are many more spins in the system, meaning MC sweeps will take longer to complete since one MC sweep checks whether a spin should flip N times. By taking $gridsize$ to be 40 for the 3D IM, the number of total spins is $40^3 = 64000$, a similar number to the 2D IM with $gridsize = 250$ ($250^2 = 62500$).

MFT was applied to the 3D IM to find projected magnetic susceptibility and magnetism. A reduced temperature ($t = (T_0^{3D} - T_c^{3D})/T_c^{3D}$) was found, and relationships described in [Rostami, 2025] were used:

$$\chi \propto t^{-\gamma},\ (H = 0),\ \gamma_{\mathrm{MFT}} = 1, \tag{7a}$$

$$m \propto t^{\beta},\ (T_0^{3D} < T_c^{3D},\ H = 0),\ \beta_{\mathrm{MFT}} = 0.5, \tag{7b}$$

where H is the magnetic field, which was taken as zero for simplicity, and β is not to be confused with inverse temperature β. These were used in python to produce a csv for 300 values of temperature for $2.5 \leq T_0^{3D} \leq 5.5$.

2.5 Reaching equilibrium

Before observing the trends of properties of the IM, it is essential to ensure that the system has reached equilibrium. This implies that the properties of the IM exhibit minimal fluctuations between MC sweeps, indicating the system is in a "steady state". Since the IM is initialised with all spins pointing downward, a single MC sweep is insufficient for the system to reach equilibrium.

To allow the system to reach equilibrium, a number of initial sweeps, denoted n_0, must be performed. The value of n_0 is determined by analysing the number of sweeps required for stabilisation. Once equilibrium is achieved, measurements are collected over $m = 30$ independent samples. This choice of m satisfies the conditions of the central limit theorem, allowing the assumption that sample means are normally distributed.

To ensure statistical independence between measurements, the system is allowed to evolve for n sweeps between each recorded sample. Like n_0, the value of n must be chosen carefully to ensure that the system forgets its previous state before the next measurement is made.

To approximate the number of sweeps before the system is in equilibrium, measures of energy and magnetism are made for different temperatures. It can be seen in Figure 3 that the model reaches equilibrium after $e^6 \approx 400$ sweeps for most values of T_0. However, magnetism does not converge within 1000 sweeps for $T_0 = 2.25$. This temperature is very close to the critical temperature of the 2D square IM ($T_c \approx 2.269$) which may be influencing the rate of convergence to equilibrium.

To further investigate this, the behaviour of the IM with $T_0 = 2.3$ and $gridsize = 250$ was observed using the graphical representation (see Figure 1). Blue islands were observed, which grew in size and quantity.

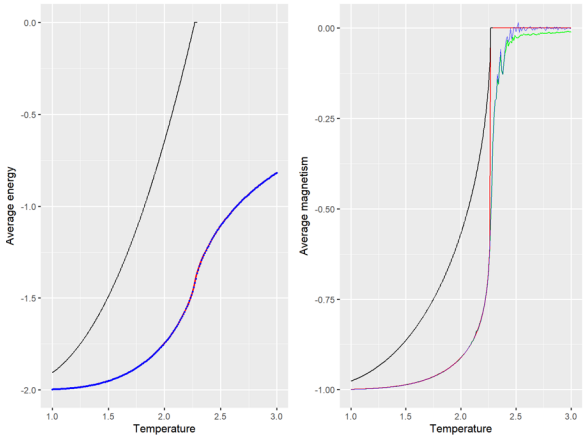

Figure 5: Average energy and magnetism for different temperatures. Red line shows the exact data calculated using Onsager's solution. Black shows predictions from MFT. Blue represents the data from the simulated IM, with $gridsize = 250$, green shows the modulus magnetism. Temperatures between 1 and 3.

After 10000 sweeps, the dominant colour of the system changed, indicating a second-order phase transition. This was verified by printing the magnetism, which was indeed positive.

Ideally, simulations would run long enough to capture such transitions regardless of when they occur. However, near the critical temperature, these transitions can require more than 10000 sweeps. To balance accuracy and efficiency, n_0 was scaled based on temperature using Onsager's exact solution for heat capacity:

$$n_0 = 3000c(T_0) + 400. \tag{8}$$

Here, $c(T_0)$ is the specific heat at temperature T_0. This scaling is justified because heat capacity is proportional to energy fluctuations and peaks sharply at T_c. The additional constant (400) provides a baseline to ensure convergence across all temperatures. At $c(2.27) = c_{max} = 3.6164$, there are $n_0 = 3000 \times 3.6164 + 400 = 11249$ sweeps, representing the maximum of n_0. This value is comparable to the number of sweeps required for the IM to undergo a polarisation flip at $T_0 = 2.3$, suggesting that the equation provides a reasonable estimate for achieving equilibrium.

Similarly, the number of sweeps between measurements, n, is also increased near the critical region to ensure independence across transitions:

$$n = 300c(T_0) + 20. \tag{9}$$

Figure 4 shows that the energy of the 3D IM reached equilibrium within 1000 sweeps, but magnetism (like in the 2D case) did not. Since there are no found exact solutions to the heat capacity for the 3D IM, values for waiting sweeps are estimated. n_0^{3D} was estimated to be 2000 and n^{3D} to be 50.

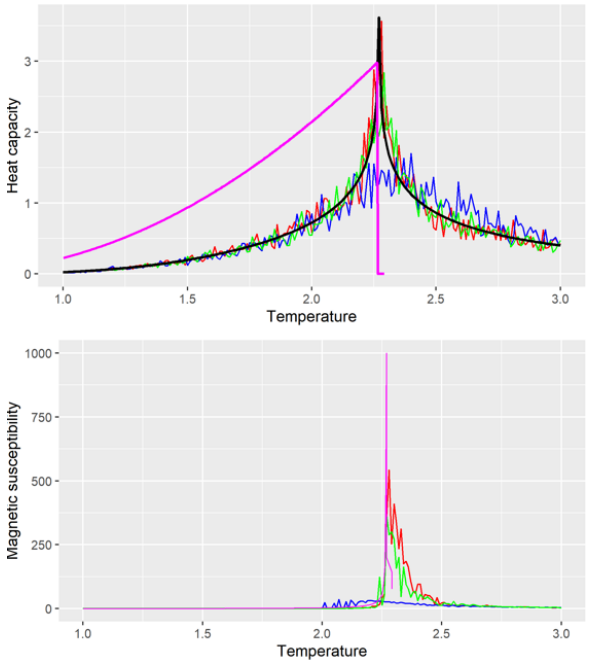

Figure 6: Heat capacity (top) and magnetic susceptibility (bottom) for grid sizes 10 (blue), 50 (green), and 250 (red). Black line in shows the exact data calculated using Onsager's solution. Pink line shows the MFT predictions. Temperatures between 1 and 3.

3 Results

As previously mentioned, Onsager solved the 2D square IM in 1944. This enabled comparison between simulation results and the exact values for the IM. Predictions from Onsager's solution are exactly calculable, which enables direct comparison for energy, magnetism, and heat capacity.

The behaviour of the IM at the critical temperature is of particular interest, where second-order phase transitions occur. Therefore the behaviour of the IMs for temperatures close to the critical temperature (from 1 to 3 for the 2D case and from 2.5 to 5.5 for the 3D case) were focused on.

With a grid size of 250, the energy simulations conformed well with the exact solution (see Figure 5). Energy increased at a slower rate after reaching T_c, and it did not reach a maximum by $T_0 = 3$. The MFT predictions did not resemble the exact solution very well, although it captured the increase in gradient at the critical temperature.

Simulated values of magnetism deviated from the exact solution more so than energy. At T_c, the exact (red) magnetism curve bends sharply, with its slope dropping from steeply positive to zero. Modulus magnetism only deviated from magnetism after the critical temperature, and had a greater amplitude once it deviated. MFT accurately predicted the point of critical temperature, but struggled to conform to magnetism for low temperature.

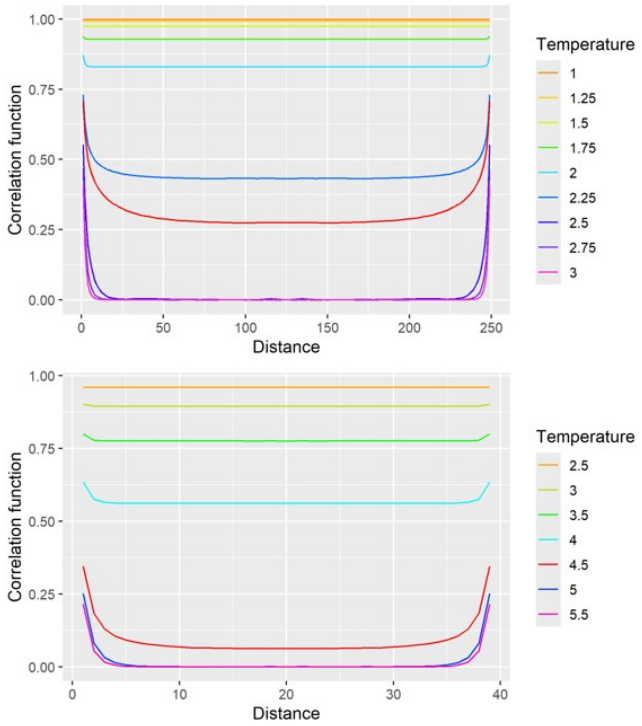

Figure 7: The correlation function per spin pair for varying temperature, 30 repeats. 50 different distances from 1 to 249 measured for 2D, all 39 distances between 1 and 39 for 3D. Critical temperature highlighted in red in both cases.

The exact heat capacity (black) shown in Figure 6 displays a sharp peak at the critical temperature. This behaviour is reflected by specific heat capacity calculated in simulations, however the peak in heat capacity is lower and less sharp for all grid sizes. As the grid size grows, the peak heat capacity slightly increases. At the largest grid size, 250, there is good conformity to the exact data. MFT badly represents the heat capacity, though it does capture the location of the critical temperature.

Since magnetic susceptibility diverges to infinity at the critical temperature in the exact solutions, it cannot be graphically compared to the simulated values. The simulated values of magnetic susceptibility spiked for temperatures greater than the critical temperature (see Figure 6). This is also shown in Figure 5, by the slow conformity to exact solutions for magnetism. The peak in magnetic susceptibility is significantly dependent on grid size. The peak grows from $\chi_{max} \approx 30$ at grid size $= 10$ to $\chi_{max} > 500$ at grid size 250. MFT does a good job here of capturing the critical temperature.

Spin pairs have high correlation at low temperatures (see Figure 7), indicating a high degree of order. In contrast, at high temperatures, spin pairs exhibit low correlation, especially at large distances, where correlation is zero. At the critical temperature (red), the system displays long range correlations that decay slowly with distance.

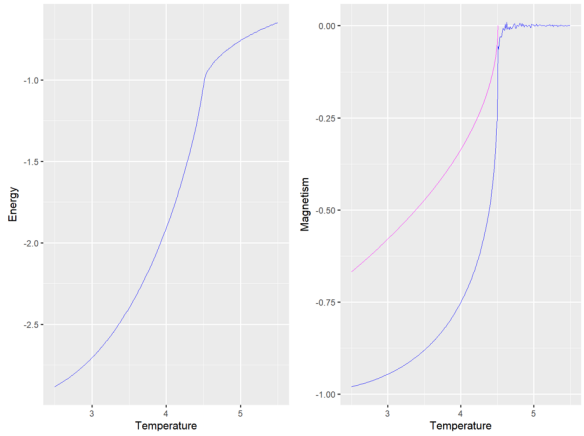

Figure 8: Blue line represents average energy and magnetism for the 3D Ising model. Temperatures between 2.5 and 5.5 in steps of 0.01, $gridsize = 40$, 30 measurements. Pink line represents MFT predictions for magnetism for the 3D IM.

3.1 3D Ising model results

Energy for the 3D IM followed a mostly smooth path for temperatures between 2.5 and 5.5 (see Figure 8). A distinguishable characteristic between the 3D and 2D IM energy is that at $T_0^{3D} \approx 4.5$, the curve sharply bent. Also of note is the lack of major fluctuations in the data, suggesting equilibrium was reached.

Magnetism of the 3D IM followed a similar trend to the 2D case (see Figure 8). There was a high positive gradient before the critical temperature, followed by a drop to zero gradient after the critical temperature. There was some variance from zero magnetism after the critical temperature, but this reduced with increased temperature. MFT gives higher magnetism for temperatures just below T_c^{3D}, however it agrees with the critical temperature found in simulations.

Heat capacity of the 3D IM dropped more sharply after the critical temperature than the 2D case (see Figure 9). Remembering that heat capacity showed some dependency on grid size in the 2D case, it is difficult to determine if the magnitude of the heat capacity is correct.

Magnetic susceptibility of the 3D IM shows signs of a second-order phase transition at the estimated critical temperature of 4.5, similar to the 2D case (see Figure 9). MFT strongly agrees with the simulated values of magnetic susceptibility, and it finds a similar critical temperature to simulations.

The correlation function of the 3D IM is seen in Figure 7 to be similar to the 2D case. At the critical temperature, the system displayed correlations over a long range, which decayed slowly with distance. At low temperatures, there was high correlation and at high temperatures there was low correlation. Notably, there is a lower correlation for temperatures close to the critical temperature estimates than the 2D case.

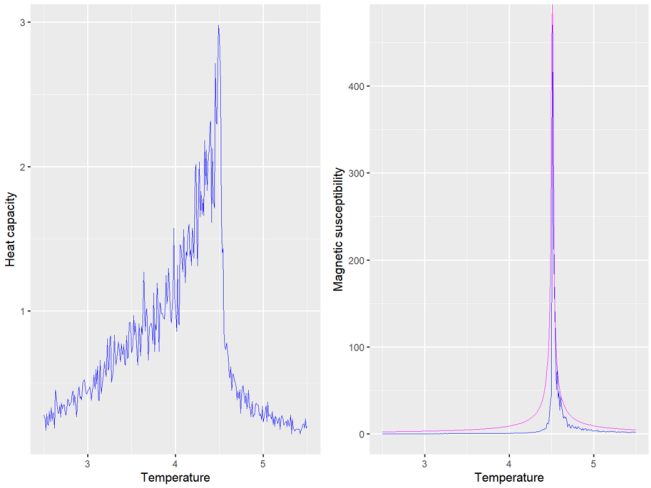

Figure 9: Blue line represents the average heat capacity (left) and magnetic susceptibility (right) for the 3D Ising model. Temperatures between 2.5 and 5.5 in steps of 0.01, $gridsize = 40$, 30 measurements. Pink line represents MFT predictions for magnetic susceptibility for the 3D IM.

4 Analysis

For the 2D IM, energy simulations showed good conformity, while magnetism exhibited larger deviations, particularly near and below T_c. This discrepancy can be attributed to finite size effects, which are known to impact measurements of magnetism in finite systems, as long range order cannot fully develop.

The behaviour of the heat capacity provided a strong indicator of the second-order phase transition. Although the simulated heat capacity peaks were broader and lower than the exact sharp peak, increasing the system size improved the sharpness and height of the peak, illustrating the effectiveness of larger grid sizes. Magnetic susceptibility similarly showed grid size dependent behaviour, with susceptibility peaks growing with increased grid size. This trend validates the prediction that susceptibility diverges at the critical point in infinite systems.

The MFT comparisons highlight its limitations: while it successfully predicted the location of the critical temperature and the general trend of observables, it consistently failed to reproduce the finer details, particularly the continuous nature of the phase transition.

Correlation function analysis provided further evidence of critical behaviour. Below T_c, strong correlations persisted across the system, reflecting ordered spin states, whereas above T_c, correlations rapidly diminished, indicative of disordered phases. Near T_c, long range correlations appeared, with spin neighbour correlations decaying slowly with distance. From this, we can predict that the critical temperature is the point after which correlations dissipate in the infinite size grid, consistent with Onsager's predictions.

In the 3D IM, similar trends were observed. Energy and magnetism behaved similarly to the 2D case, with smooth energy variation and sharp changes in magnetism at the estimated critical temperature ($T_c^{3D} \approx 4.5$). Heat capacity and magnetic susceptibility spikes further confirmed the presence of a second-order phase transition.

Correlation of spin pairs in the 3D IM was lower at the critical temperature than it was for the 2D IM. A possible explanation for this is that the system was yet to reach an equilibrium point, meaning long range order had not been established yet. This is a limitation of the 3D case, as long range order near the critical temperature may take more sweeps to achieve. However it is clear that near the critical temperature, there was still some degree of correlation in spin pairs that persisted over long distance, proving showing that long range order still occurs at the critical temperature for the 3D case.

The 3D simulations demonstrated that while larger grid sizes would be necessary to fully capture the infinite system behaviour, the critical phenomena and temperature dependent behaviours were clearly visible even for moderate grid sizes. MFT continued to approximate critical temperatures well but failed to replicate the detailed behaviour.

For this reason, it is often more informative to simulate the 3D IM directly rather than relying solely on MFT. While MFT provides valuable insights into the behaviour of the 3D IM at the critical temperature, simulations offer a more accurate representation of the model across a broader range of temperatures. However, even with a relatively modest grid size of 40, results indicated that equilibrium had not yet been achieved. For larger grid sizes, the computational demands increase significantly, requiring more sweeps to reach equilibrium and highlighting the challenges of simulating higher dimensional IMs near criticality. Consequently, a combined approach that makes use of both MFT and simulations offers the most effective strategy for studying the behaviour of the 3D IM.

5 Conclusion

Through the simulation and analysis of the 2D IM, computational methods were used to replicate known solutions. The Metropolis Monte Carlo algorithm enabled the exploration of temperature dependent behaviours such as energy, magnetism, heat capacity, and magnetic susceptibility, with results showing clear evidence of a second-order phase transition near the known critical temperature ($T_c = 2.269$). However, the MC method could have been replaced by a more efficient one, such as the Wolff algorithm. This would have allowed for faster computations and hence more sweeps to ensure equilibrium was met.

While simulated energy closely matched analytical predictions, discrepancies in magnetism and susceptibility highlighted the limitations imposed by finite size effects and computational constraints near T_c. The derivation of adaptive parameters for reaching equilibrium and measurement, particularly around T_c, proved effective in improving the model's efficiency without substantial loss of accuracy. The strong agreement between the 2D simulation results and the exact solution provided a solid foundation for applying the same methods to the more complex, three dimensional IM.

The 3D extension of the model displayed similar behaviour to the 2D case. Although no exact analytical solution exists in 3D, the temperature dependent trends in energy, magnetism, heat capacity, and susceptibility all showed clear signs of a second-order phase transition. The behaviour around the critical point mirrored that of the 2D model, with increased fluctuations and sharp changes in observables. MFT also supported the 3D predictions, although since there are no exact solutions to the 3D IM, it is hard to say how accurate simulations were. To increase confidence in the simulation results, grid size could have been increased and more sweeps could have been performed to ensure the system was in an equilibrium state.

References

Ising, E., 1925. Beitrag zur theorie des ferromagnetismus. *Zeitschrift für physik* [Online], 31, pp.253–258. Available from: https://doi.org/10.1007/BF02980577.

Onsager, L., 1944. Crystal statistics. i. a two-dimensional model with an order-disorder transition. *Phys. rev.* [Online], 65 (3-4), pp.117–149. Available from: https://doi.org/10.1103/PhysRev.65.117.

Rostami, H., 2025. *Phase transitions*. Lecture notes, PH40073 – Mathematical Physics, University of Bath, 3 February 2025.